Pediatr Radiol (2017) 47:169–177
DOI 10.1007/s00247-016-3741-5

ORIGINAL ARTICLE

Magnetic resonance tissue phase mapping demonstrates altered left ventricular diastolic function in children with chronic kidney disease

Charlotte Gimpel[1] · Bernd A. Jung[2] · Sabine Jung[3] · Johannes Brado[4] · Daniel Schwendinger[5] · Barbara Burkhardt[6] · Martin Pohl[1] · Katja E. Odening[4] · Julia Geiger[7,8] · Raoul Arnold[9]

Received: 3 June 2016 / Revised: 26 September 2016 / Accepted: 20 October 2016 / Published online: 13 December 2016

Abstract
Background Echocardiographic examinations have revealed functional cardiac abnormalities in children with chronic kidney disease.
Objective To assess the feasibility of MRI tissue phase mapping in children and to assess regional left ventricular wall movements in children with chronic kidney disease.
Materials and methods Twenty pediatric patients with chronic kidney disease (before or after renal transplantation) and 12 healthy controls underwent tissue phase mapping (TPM) to quantify regional left ventricular function through myocardial long (Vz) and short-axis (Vr) velocities at all 3 levels of the left ventricle.
Results Patients and controls (age: 8 years—20 years) were matched for age, height, weight, gender and heart rate. Patients had higher systolic blood pressure. No patient had left ventricular hypertrophy on MRI or diastolic dysfunction on echocardiography. Fifteen patients underwent tissue Doppler echocardiography, with normal z-scores for mitral early diastolic (V_E), late diastolic (V_A) and peak systolic (V_S) velocities. Throughout all left ventricular levels, peak diastolic Vz and Vr (cm/s) were reduced in patients: Vz_{base} -10.6±1.9 vs. -13.4±2.0 ($P<0.0003$), Vz_{mid} -7.8±1.6 vs. -11±1.5 ($P<0.0001$), Vz_{apex} -3.8±1.6 vs. -5.3±1.6 ($P=0.01$), Vr_{base} -4.2±0.8 vs. -4.9±0.7 ($P=0.01$), Vr_{mid} -4.7±0.7 vs. -5.4±0.7 ($P=0.01$), Vr_{apex} -4.7±1.4 vs. -5.6±1.1 ($P=0.05$).
Conclusion Tissue phase mapping is feasible in children and adolescents. Children with chronic kidney disease show significantly reduced peak diastolic long- and short-axis left ventricular wall velocities, reflecting impaired early diastolic filling. Thus, tissue phase mapping detects chronic kidney disease-related functional myocardial changes before overt left ventricular hypertrophy or echocardiographic diastolic dysfunction occurs.

Keywords Adolescents · Cardiac imaging technique · Cardio renal syndrome · Chronic renal failure · Left ventricular dysfunction · Magnetic resonance imaging · Tissue phase mapping

✉ Charlotte Gimpel
Charlotte.Gimpel@uniklinik-freiburg.de

[1] Department of General Pediatrics, Adolescent Medicine and Neonatology, Center for Pediatrics, Medical Center - University of Freiburg, Mathildenstr. 1, 79106, Freiburg, Germany

[2] Institute of Diagnostic, Interventional and Pediatric Radiology, Inselspital Bern, Bern, Switzerland

[3] Department of Nuclear Medicine, Medical Center - University of Freiburg, Freiburg, Germany

[4] Department of Cardiology and Angiology I, University Heart Center Freiburg, Freiburg, Germany

[5] University Children's Hospital Zurich, Zurich, Switzerland

[6] Pediatric Heart Center, University Children's Hospital Zurich, Zurich, Switzerland

[7] Department of Radiology, University Children's Hospital Zurich, Zurich, Switzerland

[8] Department of Radiology, Northwestern University, 737 N. Michigan Ave., Chicago, IL, USA

[9] Department of Pediatric and Congenital Cardiology, University Hospital Heidelberg, Heidelberg, Germany

Introduction

Death from cardiovascular causes largely accounts for the significant increase in mortality of patients with chronic kidney disease [1, 2]. This is especially true for young adults with childhood-onset chronic kidney disease [3], even though they do not have classical risk factors such as atherosclerosis or diabetes. Early identification and prevention of chronic kidney disease-related cardiovascular changes is, therefore, an important part of improving patient outcomes [4].

Left ventricular hypertrophy is a well-established risk marker in this population, which confers an increased risk for cardiovascular events and mortality [5, 6]. Children and adolescents with renal disease have been shown to have a high incidence of overt left ventricular hypertrophy, especially if undergoing renal replacement therapy [7, 8] but also in milder stages of chronic kidney disease [9]. Also, echocardiographic studies have demonstrated several functional abnormalities including both diastolic [10–12] and systolic contractile dysfunction [13–16]. Regional diastolic long-axis velocities, which are closely correlated to diastolic function independently of loading conditions [17], have also been measured by tissue Doppler imaging in this group suggesting diastolic dysfunction [18–21]. However, ventricular wall motion on tissue Doppler echocardiography cannot be assessed in all parts of the left ventricle, nor in all directions (along the short axis, long axis and rotational motion) and is hampered by low reproducibility [22].

Magnetic resonance tissue phase mapping is a relatively novel technique to accurately track wall motion throughout the cardiac cycle with high temporal resolution; additionally, it maps all directions of the Cartesian and intracardiac coordinate system in all parts of the ventricles [23]. Spatial resolution of tissue phase mapping has improved over time to enable imaging of smaller subjects with an acceptable scan time. However, experience of tissue phase mapping in children is only just emerging [24, 25] and published studies have included patients around the age of 50 [26–30] and volunteers only from the age of 19 years [31–34]. Also, tissue phase mapping has not been previously used in patients with renal insufficiency.

This study sought to establish whether tissue phase mapping measurements are feasible in children and adolescents and to quantify motion abnormalities seen in a chronic kidney disease population without other cardiovascular risk factors in order to isolate changes that are attributable to uremic cardiomyopathy.

Material and methods

Patients and controls

Patients were children and adolescents with chronic kidney disease stage 3 or higher (i.e. with an estimated glomerular filtration rate [GFR] below 60 ml/min*1.73 m^2) and/or who had undergone renal transplantation. None was on dialysis. The control population consisted of healthy children without a history or symptoms of cardiovascular or pulmonary disease. All volunteers had normal blood pressure at the time of MRI and no history of hypertension or renal disease. All participants were in sinus rhythm. The presence of functional and structural anomalies of the heart, cardiac valves and great vessels was an exclusion criterion. Additionally, children with pacemakers or other metallic foreign bodies were excluded. Prior written informed consent was obtained from all parents (and adolescents where appropriate). The study procedures were in accordance with the 1964 Declaration of Helsinki and its later amendments and the study protocol was approved by the ethics committee of the University of Freiburg and registered in the German registry of clinical trials (Deutsches Register Klinische Studien, trial no. DRKS00003295).

MR imaging technique and data analysis

Cardiac magnetic resonance scans were performed without sedation or application of contrast medium on a 1.5-Tesla scanner (TIM-Symphony; Siemens, Erlangen, Germany). Details of cardiac MRI acquisition for left ventricular mass and volume measurements have been described before [35]. In addition, three short-axis slices were acquired at basal, midventricular and apical levels with a black-blood prepared prospectively echocardiogram-gated gradient-echo tissue phase mapping sequence with the following settings: repetition time (TR) 5.1 ms, echo time (TE) 4.2 ms, slice thickness 8 mm, temporal resolution 24.4 ms, matrix 160 × 80, spatial resolution 2.0 × 3.1 mm^2 (interpolated to 2.0 × 2.0 mm^2), velocity sensitivity *venc* 0.2 and 0.3 m/s for in-plane and through-plane encoding, respectively. The slices were positioned on a long-axis view about 25% (basal), 50% (mid) and 75% (apical) of the distance between valve plane and apex. Through-plane motion cannot be taken into account. Spatiotemporal k-t GRAPPA (Generalized Autocalibrating Partially Parallel Acquisition) with a reduction factor of 5 was used for acceleration of data acquisition [36], yielding a scan time of 16–20 s (depending on heart rate) during breath-hold.

After manual tracing of the epi- and endocardial contours, data were further processed with a tool developed in Matlab (The MathWorks, Natick, MA) to convert velocity components from a Cartesian coordinate system into an internal polar coordinate system positioned at the center of the left ventricle. Thus, radial velocity (short-axis contraction and expansion), circumferential velocity (short-axis rotation) and long-axis velocity (long-axis shortening and lengthening) could be computed over the entire cardiac circle (Fig. 1). For each velocity, the peak velocity and time-to-peak were calculated for systole and diastole. For regional analysis, velocity components were either determined over the appropriate slice (base, midventricular or

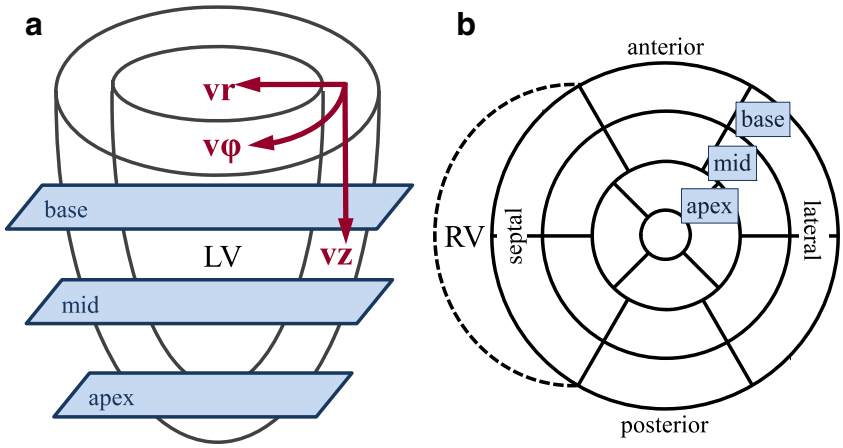

Fig. 1 Models of the left ventricle. **a** A schematic illustrates radial/short-axis (Vr), long-axis (Vz) and rotational velocities (Vφ). **b** A bull's-eye plot shows 16 segments of the left ventricle according to the American Heart Association model

apex) or the corresponding segment in the 16-segment model of the heart of the American Heart Association [37]. For easier visualization, results of the 16-segment model are displayed as bull's-eye plots (Fig. 1).

Echocardiography

On the same day as cardiac MRI, a 2-D-guided M-Mode echocardiography was performed in 15 patients according to the standards of the American Society of Echocardiography [23] by an examiner with extensive experience in echocardiography (RA, 22 years) on a Vivid 7 Dimension cardiovascular US system (GE Healthcare, Milwaukee, WI). Pulsed-wave Doppler studies at the tip of the mitral valve leaflet included mitral valve peak flow velocity in the early diastole (E) and peak velocity at atrial contraction (A). Additionally, the ratio between them (E/A) was calculated and normal values applied to screen for diastolic dysfunction [38, 39]. To quantify longitudinal myocardial function, color-coded tissue velocity cine loops were acquired from the apical four-chamber view. Narrow scan sectors were used to achieve a rate of 180–240 color Doppler frames per s and Nyquist limits were adjusted for each loop according to the actual velocity range. Cine loops were stored digitally and analyzed offline (EchoPAC Dimension 6.1; GE Healthcare Technologies Ultrasound, Horten, Norway). The following parameters were extracted from the lateral left ventricular wall, close to the mitral valve anulus: peak systolic (V_S), early diastolic velocity (V_E), and late diastolic velocity (V_A) and corresponding reference values applied for z-score calculation [40].

Clinical measurements

Patients presented for clinical examination, echocardiography, blood pressure and laboratory measurement on the same day as the cardiac MRI. The following blood parameters were measured: serum creatinine, cystatin C, bound urea nitrogen, standard blood count and electrolytes, parathyroid hormone, 25-OH-Vitamin D, N-terminal pro brain natriuretic peptide, renin and aldosterone (in supine position). Spot urines were used to quantify proteinuria as total protein/creatinine ratio. A large up-to-date German reference study was used for normal values of clinic blood pressure and anthropometric measurements [41].

Statistics

Shapiro-Wilk testing revealed normal distribution for the great majority of velocity parameters (except Vz systolic time-to-peaks); thus, parametric statistics were used. Group comparisons were made using the chi-square test for categorical variables and unpaired Student's *t*-test for continuous variables. Corrected *P*-values were adjusted for multiple testing of systolic and diastolic V_z and V_r amplitudes at 3 heart levels using the bootstrap method of Storey and Tibshirani with 100,000 resamples. Correlations are quantified by giving Spearman's rank order correlation coefficient. Throughout, *P*-values less than 0.05 were considered significant. Statistical analyses were performed using SAS V9.4 (SAS Institute, Cary, NC).

Results

Patient characteristics

Twenty-eight patients consented to take part in the study after meeting the inclusion criteria; however, two patients withdrew due to unexpected claustrophobia in the scanner. Six studies were not analyzable for technical reasons or because of motion artifacts. Patients with incomplete studies did not differ with respect to age or gender to the rest of the patients (mean age: 15.2 ± 2.2 vs. 13.3 ± 2.9 years; 50% vs. 55% females).

Anthropometric data of patients and controls are compared in Table 1 and did not differ. Despite antihypertensive treatment in 16 patients (80%), mean systolic blood pressure was still higher in the patient group (Table 1). Ambulatory blood pressure measurement revealed uncontrolled hypertension in only 2 patients (10%) with group mean 24-h blood pressure

Table 1 Anthropometric characteristics and left ventricular volume measurements on cardiac MRI, mean ± standard deviation (range) of patient and control groups

	Patients (n=20)		Controls (n=12)	
Female	n=11	(55%)	n=8	(67%)
Age (years)	13.3±2.86	(8.26 to 17.7)	13.3±4.01	(9.16 to 19.9)
Height (cm)	152±15.7	(124 to 174)	154±13.9	(135 to 173)
Weight (kg)	47.8±16.4	(25.3 to 75.2)	47.3±15.8	(25.0 to 77.0)
BSA (m^2)	1.41±0.31	(0.96 to 1.90)	1.41±0.30	(0.97 to 1.92)
BMI (kg/m^2)	20.1±3.62	(14.7 to 27.2)	19.4±3.50	(13.5 to 25.7)
Heart rate (min^{-1})	73.7±12.2	(56 to 100)	79.1±13.7	(53 to 100)
Systolic BP (mm Hg)	118±13.4*	(100 to 152)	105±9.95	(90 to 122)
Diastolic BP (mm Hg)	63.1±9.8	(47 to 90)	59.4±6.53	(49 to 71)
Pulse pressure (mm Hg)	54±11.4**	(34 to 90)	45.3±8.4	(30 to 58)
Systolic BP z-score	0.62±1.08**	(−0.53 to 3.83)	−0.37±1.05	(−2.7 to 1.50)
Diastolic BP z-score	−0.53±1.41	(−2.80 to 3.35)	−0.98±0.92	(−2.4 to 0.20)
LV mass per BSA (g/m^2)	60.8±11.8	(42.7 to 84.3)	56.3±9.49	(44.6 to 69.7)
LV end diastolic volume per BSA (ml/m^2)	73.3±11.6	(49.6 to 99)	73.2±9.49	(56.2 to 91.6)
LV end systolic volume per BSA (ml/m^2)	25.5±7.88	(15 to 49.9)	27.4±6.99	(16.2 to 43.8)
Cardiac output per BSA (ml/min per m^2)	3.48±0.83	(2.41 to 5.33)	3.42±0.88	(1.8 to 4.94)
LV ejection fraction (%)	65.4±7.61	(39.8 to 75.2)	62.8±6.17	(52.2 to 71.2)

BMI body mass index, *BP* blood pressure, *BSA* body surface area, *LV* left ventricular

*P<0.01, ** P<0.05 compared to controls

114/66 mm Hg (mean z-score: +0.22/−0.13). Calcium channel antagonists were taken by 12 patients, angiotensin converting enzyme inhibitors or angiotensin II antagonists by 11, β-blockers by 9 and diuretics by 4 patients.

The underlying renal disease was congenital hypoplasia/dysplasia of the kidneys in 8 patients (40%), glomerular disease in 7 cases (35%) and tubulointerstitial or cystic disease in 5 (25%). Mean creatinine clearance was 50 ± 23 ml/min*1.73 m^2 among pre-transplant patients and 65 ± 24 among transplanted patients (not significant). Mean protein/creatinine ratio in spot urine was 0.47 ± 0.61 g/g (0.06–2.03), with 6 children (30%) having small proteinuria and 1 nephrotic-range proteinuria (5%). Seven patients (35%) were treated for renal anemia, with mean hemoglobin of 12.3 ± 1.4 g/dl (9.7 to 14.4 g/dl). Thirteen patients (65%) had undergone kidney transplantation, all of whom received immunosuppression with a calcineurin inhibitor and mycophenolate mofetil, and 9 also received corticosteroids.

Conventional assessment of cardiac function

In a conventional cardiac MRI performed immediately prior to tissue phase mapping, there was no difference between patients and controls regarding left ventricular mass, end-diastolic and end-systolic volume, ejection fraction and cardiac output (Table 1) as well as the corresponding z-scores (data not shown). None of the patients had left ventricular hypertrophy (mean left ventricular mass z-score: 0.36 ± 0.89 [−1.1 to 1.86]) as defined by normal values by Kawel-Boehm et al. [42]. One patient had reduced ejection fraction on cardiac MRI (mean: 65.4 ± 7.6%, range: 40.0–75%).

Same-day echocardiography showed a mildly reduced ejection fraction in 2 patients (mean: 66.2 ± 6.0%, range: 52.0–75.0). Importantly, no patient had evidence of diastolic dysfunction on pulse wave Doppler (mean mitral E/A ratio: 1.99 ± 0.35, range: 1.39 to 2.64) [39]. Tissue Doppler imaging was available for 15 patients, who did not differ in age, height, weight, renal function or transplantation status from 5 patients in whom it had not been performed. Only one patient had a mitral V_E z-score value below the normal range, but all other values did not show evidence of diastolic dysfunction (mean mitral V_E z-score: −0.50 ± 1.13, range: −2.57 to 1.77 mitral V_A z-score −0.26 ± 0.83, range: −1.59 to 1.34 and mitral V_S z-score 0.09 ± 0.96, range: −1.80 to 1.64, no significant differences).

Comparison of tissue phase mapping in patients vs. controls

The most prominent difference between patients and controls were smaller peak diastolic velocities both in the short and long-axis direction and at base, midventricular and apical level (Table 2). Figure 2 shows the differences of peak diastolic velocities in each of the 16 segments of the left ventricle. Even though some segments did not reach statistical significance, there is no clear pattern of sparing. The peak systolic short-axis velocities were also significantly reduced at base and midventricular level, but this did not remain significant after adjusting for multiple testing (Table 2). There were no

Table 2 Systolic and diastolic amplitudes, mean ± standard deviation, in cm/s of ventricular wall motion in the direction of the long axis (Vz) and short axis (Vr) at heart base and apex as well as midventricular level

Peak velocities			Patients (n=20)	Controls (n=12)	P-value[1]	Adjusted P-value[1]
Systolic	Vz	base	6.03±2.4	6.81±1.9	0.34	0.96
		mid	4.95±1.5	5.76±1.8	0.17	0.75
		apex	3.45±1.0	3.88±1.5	0.33	0.95
	Vr	base	2.95±0.4	2.60±0.2	0.005	0.13
		mid	2.89±0.5	2.62±0.2	0.04	0.45
		apex	2.31±0.5	2.35±0.3	0.79	0.34
Diastolic	Vz	base	−10.6±1.9	−13.4±2.0	0.0003	0.0035
		mid	−7.8±1.6	−11±1.5	<0.0001	0.0007
		apex	−3.8±1.6	−5.3±1.6	0.01	0.11
	Vr	base	−4.2±0.8	−4.9±0.7	0.01	0.10
		mid	−4.7±0.7	−5.4±0.7	0.01	0.096
		apex	−4.7±1.4	−5.6±1.1	0.05	0.34

[1] P-values are for Student t-test and adjusted P-values are corrected for multiple testing using the bootstrap method

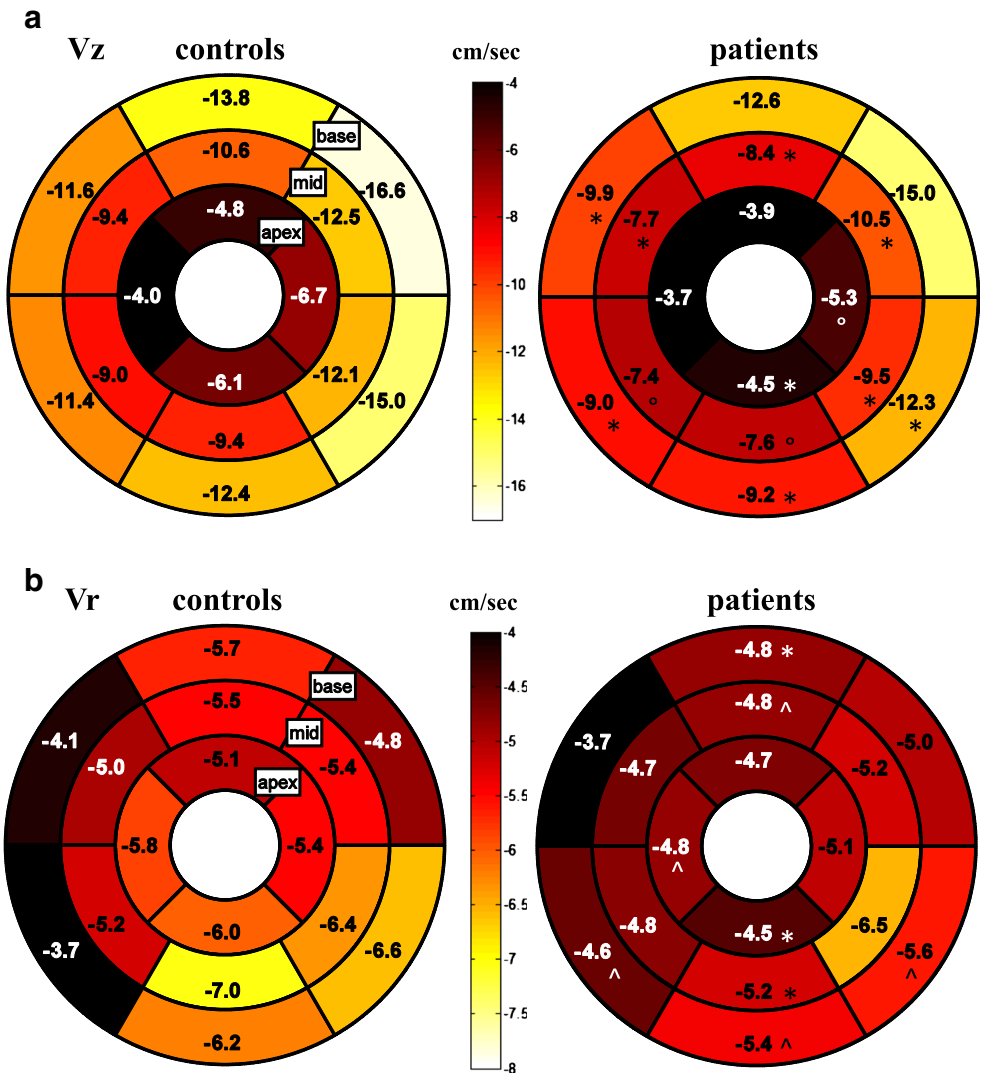

Fig. 2 Comparison of measurement in control subjects and in patients in the 16 segments of the left ventricle. **a**–**b** Diastolic amplitudes (cm/s) of ventricular wall motion in the direction of the long axis (Vz; **a**) and short axis (Vr; **b**). * $P<0.05$, ° $P=0.05$, ^ $0.06<P<0.09$

significant differences between patients and controls in the rotational velocities (Vφ) or in the time-to-peak (time-to-peaks) of all velocities on all heart levels.

Correlations of peak velocities and time-to-peak

Systolic and diastolic peak velocities in all three directions did not correlate to age, height, weight or body surface area in patients and controls. Systolic short-axis peak velocities correlated with blood pressure and pulse pressure (Table 3); however, diastolic peak velocities and systolic long-axis and rotational peak velocities did not correlate to blood pressure or heart rate. In terms of the time to reach peak velocities, all diastolic time-to-peaks showed a strong negative correlation to heart rate ($r=-0.60$ to $r=-0.76$, all $P<0.0001$), and consequently also to age, height, weight and body surface area ($r=0.40$ to 0.70, $P<0.0001$ to 0.02). The systolic time-to-peaks were correlated to heart rate less closely ($r=-0.33$ to $r=-0.53$) and correlations to anthropometric measures were also less consistent.

Correlation of velocities to left ventricular dimensions in patients

Diastolic peak long-axis and short-axis velocities showed significant correlations to cardiac MRI measurements of end-diastolic volume and left ventricular mass in patients (Table 4), but not to pro-brain natriuretic peptide. Diastolic time-to-peaks in short- and long-axis direction correlated significantly with pro-brain natriuretic peptide ($r=0.56$ to $r=0.76$, $P=0.002$ to 0.04). However, age may be a confounder here as pro-brain natriuretic peptide falls with age and was correlated to heart rate ($r=0.64$, $P=0.02$). Indeed, multiple regression analysis testing all parameters that were significantly correlated in univariate analysis, revealed that only the influence of heart rate, but not pro-brain natriuretic peptide, remained significant in models for diastolic time-to-peaks.

Correlation to kidney disease and blood pressure in the patient group

To explore the effects of the underlying renal disease with the decreased diastolic and systolic amplitudes found in patients, we analyzed correlations to disease parameters. Diastolic long-axis amplitudes were significantly correlated to both proteinuria and renin/aldosterone ratio (Table 5), but not consistently to renal function. Short-axis diastolic amplitudes did not correlate to renal function or proteinuria. Both long- and short-axis diastolic amplitudes were not correlated to pro-brain natriuretic peptide, renin, aldosterone, serum electrolytes or measures of renal anemia and secondary hyperparathyroidism.

While systolic short-axis peak velocities (which correlated to blood pressure at time of cardiac MRI in the whole group) also correlated to clinic blood pressure (taken several hours earlier) in the patients, they did not correlate to any of the 24-h blood pressure parameters (started in the evening of cardiac MRI examination). Indeed, the correlation of short-axis peak systolic velocities was stronger in controls than in patients. Systolic amplitudes were not correlated to renal function, proteinuria, pro-brain natriuretic peptide, renin, aldosterone, electrolytes, renal anemia or secondary hyperparathyroidism.

Discussion

Cardiovascular events are the leading cause of mortality in patients with both childhood- and adult-onset end-stage renal failure [1, 3]. Cardiovascular changes in these patients result from a combination of hypertension, fluid overload, abnormalities of calcium-phosphate metabolism and uremic toxins [41]. Uremic cardiomyopathy is a distinct, but not fully understood entity, which is difficult to study in adults as atherosclerotic and diabetic changes often coexist [43]. Traditionally, left ventricular mass is used as the main parameter to reflect cardiovascular damage in chronic kidney disease patients. However, uremic cardiomyopathy probably starts prior to overt left ventricular hypertrophy and MR spectroscopy has shown altered myocardial structure and decreased systolic function in pediatric chronic kidney disease patients [44].

This study assesses magnetic resonance tissue phase mapping as a novel tool to characterize cardiac wall motion with high spatial and temporal resolution in children with chronic kidney disease. Despite extending a normal cardiac MRI examination by about 15 min and three breath-hold maneuvers, tissue phase mapping was feasible without sedation in children as young as 8 years old. From personal experience, the

Table 3 Spearman's rank order correlation coefficients (r) and corresponding *P*-values of systolic short-axis (Vr) peak velocities to blood pressure parameters

Peak velocities				Systolic blood pressure	Diastolic blood pressure	Pulse pressure
Systolic	Vr	base	r	0.46	0.30	0.42
			P-values	0.008	0.094	0.018
		mid	r	0.47	0.28	0.56
			P-values	0.006	0.13	0.001
		apex	r	0.23	0.22	0.35
			P-values	0.22	0.23	0.047

Table 4 Spearman's rank order correlation coefficients (*r*) and corresponding *P*-values of diastolic long-axis (Vz) and short-axis (Vr) peak velocities to left ventricular dimensions[1]

Peak velocities				nEDV	nLVM
Diastolic	Vz	base	r	−0.59	−0.45
			P-values	0.008	0.056
		mid	r	−0.56	−0.46
			P-values	0.012	0.049
		apex	r	−0.49	−0.51
			P-values	0.035	0.025
Diastolic	Vr	base	r	−0.46	−0.25
			P-values	0.046	0.31
		mid	r	−0.41	−0.39
			P-values	0.08	0.098
		apex	r	−0.62	−0.69
			P-values	0.005	0.001

nEDV left-ventricular end-diastolic volume normalized to body surface area, *nLVM* left-ventricular mass normalized to body surface area

[1] Note that correlations are negative because diastolic amplitudes are given as negative values. Thus, a smaller amplitude will mean a larger numerical value

ability to cooperate with MRI examinations is more dependent on the individual child's cooperation than age. In line with this, dropouts were not significantly younger than patients with successful exams.

Previous studies have reported significant variation of tissue phase mapping findings with age and gender [33]. The healthy children reported here also showed significantly different peak velocities to adults and a high correlation of heart rate to time-to-peaks, underlining the need for a well-matched control group. Patient and control groups were well-matched for age, gender, height, weight and body surface area. Patients had higher systolic blood pressure despite antihypertensive treatment, but systolic blood pressure only correlated with systolic peak short-axis velocities but not to any diastolic velocities, which were the most prominent difference between patient and control groups; therefore, we feel it does not influence the main results.

The current group of children and adolescents with chronic kidney disease had significantly decreased peak diastolic short- and long-axis velocities compared to healthy controls. Decreased diastolic peak wall velocities represent diastolic dysfunction with reduced early diastolic filling, as they correlate well with peak early filling velocity in the isovolumic relaxation period [38, 39]. Previous echocardiographic studies have described diastolic dysfunction in children on dialysis or after transplantation [10, 18, 21] and more recently using advanced tissue Doppler or 2-D speckle tracking strain echocardiography also in children with chronic kidney disease [15, 20, 45–47]. A current study by Han et al. [48] also found diastolic dysfunction to be an independent predictor of cardiovascular events in adults with end-stage renal disease, even in the absence of diastolic heart failure or systolic dysfunction. As tissue phase mapping demonstrates diastolic changes in our cohort with normal echocardiographic diastolic function, we think that it is probably more sensitive for detecting diastolic dysfunction than conventional echocardiography.

In terms of determining main causative factors, the alterations of diastolic velocities did not correlate to blood pressure, left ventricular mass or anthropometric measures and therefore do not appear to be caused by hypertension per se. Rather, the fact that diastolic peak short-axis velocities correlated to proteinuria suggests that the kidney disease itself contributes, i.e. that these changes represent early alterations of uremic cardiomyopathy before left ventricular hypertrophy is seen. The more pronounced alteration of long-axis compared to short-axis velocities was also reported in one tissue phase mapping study of obese subjects and echocardiographic studies on asymptomatic patients and those with subclinical diabetic heart disease [26, 45, 46], suggesting that radial contraction can compensate for reduced longitudinal contraction in mild stages of diffuse

Table 5 Spearman's rank order correlation coefficients (*r*) and corresponding *P*-values of diastolic long-axis (Vz) peak velocities to renal function, proteinuria and aldosterone/renin ratio

Peak velocities				Creatinine clearance	Urinary protein/creatinine ratio	Aldosterone/Renin ratio
Diastolic	Vz	base	r	0.17	−0.59	0.67
			P-values	0.46	0.013	0.023
		mid	r	0.49	−0.54	0.64
			P-values	0.027	0.025	0.035
		apex	r	0.37	−0.37	−0.05
			P-values	0.11	0.14	0.89

myocardial disease. Thus, even though the causal role of chronic kidney disease is extremely likely due to the lack of comorbidities in this cohort, the pattern of changes is unspecific.

In addition to the diastolic changes, patients also had smaller peak systolic short-axis velocities than controls at base and midventricular level. However, this was less pronounced and did not remain significant after adjusting for multiple testing. Also, the systolic short-axis velocities were correlated to blood pressure in both patients and controls, but not to markers of renal disease. Therefore, because patients had higher blood pressure, we interpret the decreased systolic velocities as a reflection of current blood pressure rather than being related to chronic kidney disease.

The time course of systolic and diastolic contraction and relaxation, assessed as time-to-peak velocity, did not differ between patients and controls. Even though there was a consistent correlation of diastolic times-to-peak to pro-brain natriuretic peptide, this most likely reflects a common correlation of both to heart rate. Also, clinical usefulness of pro-brain natriuretic peptide is limited in this cohort due to its accumulation in renal failure.

A limitation of this study is the small cohort size, which unfortunately does not allow for subgroup analysis of patients prior to and after renal transplantation or to differentiate effects of different antihypertensive drugs. Also, the fact that no patient was on renal replacement therapy, as well as good control of hypertension and hyperparathyroidism, may obscure the influence of these factors on the cardiac pathology. Due to the high number of patients receiving combination therapy of up to five antihypertensive agents, subgroup analysis by antihypertensive drugs was also not possible. However, as the first description of tissue phase mapping in patients with chronic kidney disease, we were able to clearly detect changes even in early stages of the disease and without overt left ventricular hypertrophy. This confirms tissue phase mapping to be a sensitive tool for detecting functional cardiac motion impairments, despite the fact that echocardiography remains a cheaper and quicker alternative.

Conclusion

Cardiac tissue phase mapping is feasible in children and adolescents. In our pediatric population with moderate chronic kidney disease, normal left ventricular mass on cardiac MRI and normal diastolic function on echocardiography, tissue phase mapping revealed reduced early diastolic wall motion, suggesting that tissue phase mapping may be more sensitive in picking up diastolic dysfunction than standard echocardiography and that it is an interesting tool for the further exploration of uremic cardiomyopathy.

Acknowledgments We thank Adriana Komancsek (radiographer) and her team for the competent acquisition of cardiac MR images.

Compliance with ethical standards

Conflicts of interest None

References

1. Chronic Kidney Disease Prognosis Consortium, Matsushita K, van der Velde M et al (2010) Association of estimated glomerular filtration rate and albuminuria with all-cause and cardiovascular mortality in general population cohorts: a collaborative meta-analysis. Lancet 375:2073–2081
2. McCullough PA, Li S, Jurkovitz CT et al (2008) Chronic kidney disease, prevalence of premature cardiovascular disease, and relationship to short-term mortality. Am Heart J 156:277–283
3. Groothoff JW, Gruppen MP, Offringa M et al (2002) Mortality and causes of death of end-stage renal disease in children: a Dutch cohort study. Kidney Int 61:621–629
4. Sud M, Tangri N, Pintilie M et al (2014) Risk of end-stage renal disease and death after cardiovascular events in chronic kidney disease. Circulation 130:458–465
5. Zoccali C, Benedetto FA, Mallamaci F et al (2001) Prognostic impact of the indexation of left ventricular mass in patients undergoing dialysis. J Am Soc Nephrol 12:2768–2774
6. Shlipak MG, Fried LF, Cushman M et al (2005) Cardiovascular mortality risk in chronic kidney disease: comparison of traditional and novel risk factors. JAMA 293:1737–1745
7. Johnstone LM, Jones CL, Grigg LE et al (1996) Left ventricular abnormalities in children, adolescents and young adults with renal disease. Kidney Int 50:998–1006
8. Mitsnefes MM, Kimball TR, Witt SA et al (2003) Left ventricular mass and systolic performance in pediatric patients with chronic renal failure. Circulation 107:864–868
9. Matteucci MC, Wühl E, Picca S et al (2006) Left ventricular geometry in children with mild to moderate chronic renal insufficiency. J Am Soc Nephrol 17:218–226
10. Goren A, Glaser J, Drukker A (1993) Diastolic function in children and adolescents on dialysis and after kidney transplantation: an echocardiographic assessment. Pediatr Nephrol 7:725–728
11. Mitsnefes MM, Kimball TR, Border WL et al (2004) Impaired left ventricular diastolic function in children with chronic renal failure. Kidney Int 65:1461–1466
12. Rinat C, Becker-Cohen R, Nir A et al (2010) A comprehensive study of cardiovascular risk factors, cardiac function and vascular disease in children with chronic renal failure. Nephrol Dial Transplant 25:785–793
13. Chinali M, de Simone G, Matteucci MC et al (2007) Reduced systolic myocardial function in children with chronic renal insufficiency. J Am Soc Nephrol 18:593–598
14. Raimondi F, Chinali M, Girfoglio D et al (2009) Inappropriate left ventricular mass in children and young adults with chronic renal insufficiency. Pediatr Nephrol 24:2015–2022
15. Chinali M, Matteucci MC, Franceschini A et al (2015) Advanced parameters of cardiac mechanics in children with CKD: the 4C study. Clin J Am Soc Nephrol 10:1357–1363
16. Tafreshi RI, Human N, Otukesh H (2011) Evaluation of combined left ventricular function using the myocardial performance index in children with chronic kidney disease. Echocardiography 28:97–103

17. Ommen SR, Nishimura RA, Appleton CP et al (2000) Clinical utility of Doppler echocardiography and tissue Doppler imaging in the estimation of left ventricular filling pressures: a comparative simultaneous Doppler-catheterization study. Circulation 102:1788–1794
18. Ten Harkel ADJ, Cransberg K, Van Osch-Gevers M et al (2009) Diastolic dysfunction in paediatric patients on peritoneal dialysis and after renal transplantation. Nephrol Dial Transplant 24:1987–1991
19. Simpson JM, Rawlins D, Mathur S et al (2013) Systolic and diastolic ventricular function assessed by tissue Doppler imaging in children with chronic kidney disease. Echocardiography 30:331–337
20. Lindblad YT, Axelsson J, Balzano R et al (2013) Left ventricular diastolic dysfunction by tissue Doppler echocardiography in pediatric chronic kidney disease. Pediatr Nephrol 28:2003–2013
21. Schoenmaker NJ, Kuipers IM, van der Lee JH et al (2014) Diastolic dysfunction measured by tissue Doppler imaging in children with end-stage renal disease: a report of the RICH-Q study. Cardiol Young 24:236–244
22. Abraham TP, Dimaano VL, Liang H-Y (2007) Role of tissue Doppler and strain echocardiography in current clinical practice. Circulation 116:2597–2609
23. Petersen SE, Jung BA, Wiesmann F et al (2006) Myocardial tissue phase mapping with cine phase-contrast MR imaging: regional wall motion analysis in healthy volunteers. Radiology 238:816–826
24. Parekh K, Markl M, Magrath P et al (2014) Assessment of myocardial motion in children and young adults using high-temporal resolution MR tissue phase mapping. J Cardiovasc Magn Reson 16: P328
25. Camarda J, Magrath P, Parekh K et al (2015) Co-registered MR tissue phase mapping and speckle tracking echocardiography: inter-modality comparison of regional myocardial velocities in pediatric patients. J Cardiovasc Magn Reson 17:Q103
26. Rider OJ, Ajufo E, Ali MK et al (2015) Myocardial tissue phase mapping reveals impaired myocardial tissue velocities in obesity. Int J Cardiovasc Imaging 31:339–347
27. Föll D, Markl M, Menza M et al (2014) Cold ischaemic time and time after transplantation alter segmental myocardial velocities after heart transplantation. Eur J Cardiothorac Surg 45:502–508
28. Foell D, Jung B, Germann E et al (2013) Hypertensive heart disease: MR tissue phase mapping reveals altered left ventricular rotation and regional myocardial long-axis velocities. Eur Radiol 23: 339–347
29. Foell D, Jung BA, Germann E et al (2013) Segmental myocardial velocities in dilated cardiomyopathy with and without left bundle branch block. J Magn Reson Imaging 37:119–126
30. Codreanu I, Pegg TJ, Selvanayagam JB et al (2011) Details of left ventricular remodeling and the mechanism of paradoxical ventricular septal motion after coronary artery bypass graft surgery. J Invasive Cardiol 23:276–282
31. Codreanu I, Robson MD, Rider OJ et al (2014) Details of left ventricular radial wall motion supporting the ventricular theory of the third heart sound obtained by cardiac MR. Br J Radiol 87: 20130780
32. Codreanu I, Robson MD, Rider OJ et al (2013) Effects of ventricular insertion sites on rotational motion of left ventricular segments studied by cardiac MR. Br J Radiol 86:20130326
33. Föll D, Jung B, Schilli E et al (2010) Magnetic resonance tissue phase mapping of myocardial motion: new insight in age and gender. Circ Cardiovasc Imaging 3:54–64
34. Codreanu I, Robson MD, Golding SJ et al (2010) Longitudinally and circumferentially directed movements of the left ventricle studied by cardiovascular magnetic resonance phase contrast velocity mapping. J Cardiovasc Magn Reson 12:48
35. Arnold R, Schwendinger D, Jung S et al (2016) Left ventricular mass and systolic function in children with chronic kidney disease-comparing echocardiography with cardiac magnetic resonance imaging. Pediatr Nephrol 31:255–265
36. Bauer S, Markl M, Föll D et al (2013) K-t GRAPPA accelerated phase contrast MRI: improved assessment of blood flow and 3-directional myocardial motion during breath-hold. J Magn Reson Imaging 38:1054–1062
37. Cerqueira MD, Weissman NJ, Dilsizian V et al (2002) Standardized myocardial segmentation and nomenclature for tomographic imaging of the heart. A statement for healthcare professionals from the Cardiac Imaging Committee of the Council on Clinical Cardiology of the American Heart Association. Circulation 105:539–542
38. Schmitz L, Koch H, Bein G et al (1998) Left ventricular diastolic function in infants, children, and adolescents. Reference values and analysis of morphologic and physiologic determinants of echocardiographic Doppler flow signals during growth and maturation. J Am Coll Cardiol 32:1441–1448
39. Nagueh SF, Smiseth OA, Appleton CP et al (2016) Recommendations for the evaluation of left ventricular diastolic function by echocardiography: an update from the American Society of Echocardiography and the European Association of Cardiovascular Imaging. J Am Soc Echocardiogr 29:277–314
40. Dallaire F, Slorach C, Hui W et al (2015) Reference values for pulse wave Doppler and tissue Doppler imaging in pediatric echocardiography. Circ Cardiovasc Imaging 8:e002167
41. Neuhauser HK, Thamm M, Ellert U et al (2011) Blood pressure percentiles by age and height from nonoverweight children and adolescents in Germany. Pediatrics 127:e978–e988
42. Kawel-Boehm N, Maceira A, Valsangiacomo-Buechel ER et al (2015) Normal values for cardiovascular magnetic resonance in adults and children. J Cardiovasc Magn Reson 17:29
43. Gross M-L, Ritz E (2008) Hypertrophy and fibrosis in the cardiomyopathy of uremia–beyond coronary heart disease. Semin Dial 21:308–318
44. Weaver DJ Jr, Kimball TR, Koury PR et al (2009) Cardiac output and associated left ventricular hypertrophy in pediatric chronic kidney disease. Pediatr Nephrol 24:565–570
45. Mencarelli F, Fabi M, Corazzi V et al (2014) Left ventricular mass and cardiac function in a population of children with chronic kidney disease. Pediatr Nephrol 29:893–900
46. Dogan CS, Akman S, Simsek A et al (2015) Assessment of left ventricular function by tissue Doppler echocardiography in pediatric chronic kidney disease. Ren Fail 37:1094–1099
47. van Huis M, Schoenmaker NJ, Groothoff JW et al (2016) Impaired longitudinal deformation measured by speckle-tracking echocardiography in children with end-stage renal disease. Pediatr Nephrol 31:1499–1508
48. Han JH, Han JS, Kim EJ et al (2015) Diastolic dysfunction is an independent predictor of cardiovascular events in incident dialysis patients with preserved systolic function. PLoS ONE 10:e0118694